The Importance of Apex Location and Proximal Hemi-Curve Morphology for the Surgical Tactic of Significant Convex Coronal Imbalance in Patients with Dystrophic Scoliosis Secondary to Type I Neurofibromatosis: Classification and Management

Saihu Mao (siemens_636@163.com)
Nanjing Drum Tower Hospital, The Affiliated Hospital of Nanjing University Medical School
Song Li
Nanjing Drum Tower Hospital, The Affiliated Hospital of Nanjing University Medical School
Yanyu Ma
Nanjing Drum Tower Hospital, The Affiliated Hospital of Nanjing University Medical School
Ben-long Shi
Nanjing Drum Tower Hospital, The Affiliated Hospital of Nanjing University Medical School
Zhen Liu
Nanjing Drum Tower Hospital, The Affiliated Hospital of Nanjing University Medical School
Ze-zhang Zhu
Nanjing Drum Tower Hospital, The Affiliated Hospital of Nanjing University Medical School
Jun Qiao
Nanjing Drum Tower Hospital, The Affiliated Hospital of Nanjing University Medical School
Yong Qiu
Nanjing Drum Tower Hospital, The Affiliated Hospital of Nanjing University Medical School

Research Article

Keywords: Convex coronal imbalance, Dystrophic scoliosis, Type I Neurofibromatosis, Classification

Posted Date: August 31st, 2021

DOI: https://doi.org/10.21203/rs.3.rs-844306/v1

Abstract

Background. There was a paucity of valid information on how to discriminate between different patterns of convex coronal imbalance (CCI>3cm) in dystrophic scoliosis secondary to Type I neurofibromatosis (DS-NF1), while aggravated postoperative CCI occurred regularly with the causes being insufficiently investigated. We aimed to develop a new classification of CCI in DS-NF1, and to optimize the coronal rebalancing strategies.

Methods. NF1-related scoliosis database was reviewed and different types of CCI were identified, and the outcomes of coronal rebalance were analyzed.

Results. Two main CCI patterns were defined: thoracic CCI (Type 1) and thoracolumbar/lumbar CCI (Type 2), and were further subtyped by the compensatory behavior of the upper hemi-curve (straight or curved morphology). The incidence of immediate post-op CCI was 0.0% and 63.6% for Type1 and Type 2 groups, respectively. Mismatch of both translation and inclination correction between the upper and lower hemi-curve was significant in the post-op coronal imbalanced group (△Upper Arc Translation/△Lower Arc Translation: 109.6±60.0% vs. 31.8±34.4%, p=0.008; △Upper Arc Inclination/△Lower Arc Inclination: 89.8±36.6% vs. 33.5±37.3%, p=0.012). Multiple linear regression analysis revealed that △UAT/△LAT significantly correlated with the correction of coronal balance distance (β=-21.567; p=0.018). A surgical rebalancing algorithm was proposed to treat each subtype.

Conclusion. Thoracolumbar/lumbar CCI in dystrophic scoliosis was prone to suffer high risk of persistent post-op CCI. Satisfying coronal rebalance should rely on maximal translational correction of lower hemi-curve, while the upper hemi-curve played the role of fine-tuning for coronal realignment rather than radical Cobb correction, straight morphology in particular.

Introduction

Dystrophic scoliosis secondary to neurofibromatosis type I (DS-NF1) is characterized by distinctive bone abnormalities causing spinal instability, deformity onset and worsening[1, 2]. Extraordinary and rapid curve progression is common for juvenile patients or those exhibiting ≥ 3 dystrophic features[3]. A highly rotated short curve span often co-exists with regional kyphosis, while the coronal and sagittal malalignments are prevailing in presence of dystrophic vertebral rotatory subluxation. Trunk shift (TS) with subsequent coronal imbalance (CI) can occur in those with highly dystrophic kyphoscoliosis, especially when the curve apex locates in the thoracolumbar/lumbar regions. This represents an additional level of complexity when surgery is indicated to restore the spinal alignments.

Residual or even aggravated CI after surgery has been reported to compromise the health-related quality of life (HRQoL) and can increase the risk of implant failure[4–6]. However, how to effectively rebalance the coronal malalignment remains subject of debate. In 2016, Qiu proposed a novel classification for CI in degenerative lumbar scoliosis (DLS)[7], which indicated that type C CI with coronal balance distance ≥ 3 cm harbored high risk of immediate post-operative CI. Obeid emphasized that the rebalance of coronal

trunk for convex CI depended mainly on the correction of the lumbosacral fractional curve rather than the main curve[8]. Additionally, multiple innovative techniques have been also developed for better restoration of coronal malalignment involving the sequential correction technique, the kickstand and tie rod techniques[9–11]. All these techniques utilize the robust pelvic fixation to provide additional corrective force to obtain marked coronal rebalance.

Despite being effective, spinal-pelvic fixation is only indicated for a limited spectrum of pediatric spinal disorders mainly involving lumbosacral congenital vertebral malformations and neuromuscular scoliosis with pelvic obliquity[12, 13]. For young NF-1 dystrophic scoliosis patients whose lumbosacral discs and facet joints are not degenerated and coronally mobile, pelvic fixation is not the mainstay treatment option[14]. This will be beneficial for preserving the mobility of lumbosacral and sacroiliac joints, retaining the distal coronal compensatory capability and improving the HRQoL[8]. Thus, these aforementioned coronal rebalancing strategies, which are mainly designed for DLS, can't be applied indiscriminately to young patients with CI. This dilemma makes the complete depiction of patterns of convex CI (CCI) in dystrophic scoliosis essential for improving individualized surgical management.

From the existing literature, to the best of our knowledge, there was a paucity of valid information on how to discriminate between different patterns of CCI in DS-NF1, and the optimum coronal rebalancing strategies were insufficiently investigated. This study was designed to develop a comprehensive classification of convex coronal spinal malalignment, to identify the risk factors for persistent postoperative CI and to propose a treatment algorithm for this specific condition.

Materials And Methods

Following the Hospital Clinical Research Ethics Committee approval, this retrospective study was conducted on patients with DS-NF1 referred for corrective surgery at our institution from October 2011 to November 2018. The diagnosis of dystrophic scoliosis in NF-1 was made using established diagnostic criteria[15, 16]. Enrollment was limited to NF-1 patients with (1) dystrophic scoliosis and concomitant trunk shift causing convex coronal imbalance: coronal balance distance ≥ 3 cm; (2) intact neurological function before surgery; (3) minimum two-year follow-up with complete image data. The exclusion criteria were applied to those with (1) multiple sporadic dystrophic bone defects along the spine causing double or triple curves; (2) solitary dystrophic lesion in sacrum causing compensatory lumbar/thoracolumbar scoliosis and trunk shift; (3) presence of pelvic obliquity due to dystrophic bone defects in the lower limbs. A total 179 DS patients with NF-1 were operated during that time period, and finally, only 15 patients (age, 14.7 ± 4.4yrs; range, 10-26yrs; 7 males and 8 females; mean follow-up, 3.3± 1.5yrs) who fulfilled the inclusion and exclusion criteria were enrolled in this study. Their medical records, imaging scans, and operative reports were reviewed. The data collected include preoperative, postoperative and final main curve Cobb and kyphotic angles, patterns of convex CI, apex location, presence of vertebral rotatory subluxation (defined as a classic double-vertebrae sign on the axial computed tomography images)[17, 18], coronal balance distance (CBD), sagittal vertical axis (SVA), surgical strategies, fusion segments, implant density, ratio of laminar hook, postoperative neurological status, and surgical

complications. Curve flexibility was not assessed for this special patient subgroup. This was attributable to the potential risk of neurological impairments if side bending movements were performed hinging the unstable apical region.

Classification of convex coronal imbalance

Antagonistic role of the upper and lower hemi-curve in the formation of coronal imbalance could be easily recognized: the lower hemi-curve played the role of imbalance driver causing the trunk shifting to the convex side, whereas the upper hemi-curve served the role of imbalance compensator. CI would occur if the upper compensation was distinctly insufficient. Based on the location of curve apex and the compensatory behavior of the upper hemi-curve, four types of CCI were determined:

Type 1: Thoracic convex coronal imbalance

For Type 1 CCI, the apex located above T12, and there were sufficient non-dystrophic vertebrae (≥3) locating distal to apex. The subtypes were identified according to the morphology of the upper hemi-curve.

Type 1A: The morphology of the upper hemi-curve was straight and vertical, indicating no compensation for CCI (Fig 1a).

Type 1B: The morphology of the upper hemi-curve was curved and inclined, moving the deviated torso partially back to midline (Fig 1b).

Type 2: Thoracolumbar/Lumbar convex coronal imbalance

For Type 2 CCI, the apex located between T12 and L4. There were limited (Thoracolumbar, apex between T12-L1) or insufficient (Lumbar, apex between L2-L4) non-dystrophic vertebrae (≤3) locating distal to apex. The subtypes were identified in a similar way.

Type 2A: The morphology of the upper hemi-curve was straight and vertical (Fig 1c).

Type 2B: The morphology of the upper hemi-curve was curved and inclined (Fig 1d).

All the recruited patients were stratified according to the above-mentioned classification. The concrete distribution of each CCI type was as follows: Type 1A: 1 case (6.7%); Type 1B: 3 cases (20.0%); Type 2A: 3 cases (20.0%); Type 2B: 8 cases (53.3%). Among them, 1 patient in thoracic CCI group (Type1B) and 3 patients in thoracolumbar/lumbar CCI group (Type2B) received staged surgery with combined posterior-anterior or anterior- posterior approach (Table 1), while the rest 11 patients (73.3%) underwent posterior-only spinal instrumentation and fusion. Supplementary anterior fusion utilizing structural fibular allograft (2 patients) (Fig 3) or autogenous rib grafts (1 patient) (Fig 4) was applied when the pedicle screw density in the apical region was distinctively low due to pedicle dystrophy. Stage 1 anterior release involving intervertebral disc resection and autogenous rib grafting was performed in 1 Type 2B patient,

followed by skull-femoral traction for 2 weeks and subsequent stage 2 posterior spinal correction and fusion.

Spinal traction was indicated if Cobb angle > 90° or kyphosis > 80°. Aside from the aforementioned one Type 2 patient (9.1%), spinal traction was also applied for another 3 patients in Type 1 group (75%). Among them, two received halo-gravity traction (HGT) using a halo-wheelchair for one month, while the third one was applied with skull-femoral traction in bed for 2 weeks before posterior surgery. Posterior-only spinal instrumentation and fusion was performed with all pedicle screw or hybrid constructs, and was assisted with satellite rod technique for two patients being operated in late stage.

Radiographic assessments

The following parameters were also measured pre- and post-operatively for analysis of the separate contribution of the upper and lower hemi-curve to CI onset and prognosis: lower arc translation, upper arc translation, lower arc inclination, upper arc inclination, UIV (upper instrumented vertebra) tilt, LIV (lower instrumented vertebra) tilt, UIV translation and instrumentation mass inclination. All measurements were performed using the Surgimap spine software (Version 2.3.1.5; Spine Software, New York, NY). The definitions of the standard measuring techniques of the aforementioned parameters were defined as follows:

1. Lower arc translation (LAT, Fig. 2a): defined as the distance from the center of apex to the center sacral vertical line (CSVL).
2. Upper arc translation (UAT, Fig. 2b): defined as the distance from the center of UIV to the vertical line crossing the center of apex.
3. Lower arc inclination (LAI, Fig. 2c): defined by the angle formed between the line drawn from the center of LIV to the center of apex and the vertical line.
4. Upper arc inclination (UAI, Fig. 2d): defined by the angle formed between the line drawn from the center of UIV to the center of apex and the vertical line.
5. UIV tilt: defined as the angle formed by the line drawn parallel to the superior end plate of the UIV and the horizontal line.
6. LIV tilt: defined as the angle formed by the line drawn parallel to the superior end plate of the LIV and the horizontal line.
7. UIV translation (Fig. 2e): defined as the distance from the center of UIV to the CSVL.
8. Instrumentation mass inclination (Fig. 2f): defined by the angle formed between the line drawn from the center of UIV to the center of LIV and the vertical line.

The recruited patients were assigned into two groups according to whether or not the post-op residual CBD exceeded 3cm: the balanced group (post-op CBD <3cm) and the imbalanced group (post-op CBD ≥ 3cm). The operative changes of the translation and inclination for the upper and lower hemi-curves were recorded as △UAT, △LAT, △UAI and △LAI, respectively. Considering the antagonistic role of the upper and

lower hemi-curve in the rebalance for coronal malalignment, the ratio of △UAT/△LAT and ratio of △UAI/△LAI were both calculated, which were indicative of whether the separate corrections of upper and lower hemi-curve were matched and cooperative or mismatched and antagonistic.

Statistical Analysis

Data analysis was conducted using statistical software (SPSS 20.0, SPSS Inc., Chicago, IL). Statistical data are presented as the mean ± standard deviation. Independent-sample t test was applied to compare the deformity parameters between the balanced and imbalanced groups. Comparisons between post-op and follow-up parameters were made by paired t test. Based on our clinical experience and meanwhile to avoid the pitfall of multicollinearity between parameters, △UAI/△LAI, △UAT/△LAT, △(UIV tilt + LIV tilt) and main curve correction rate were selected to explore whether they could contribute to the correction of CBD. A p value < 0.05 was considered statistically significant.

Results

Surgical outcomes

The pre-op, post-op and final Cobb angle of main curve, kyphosis, CBD and SVA for Type1 and Type 2 groups were shown in Table 2. The incidence of CCI immediately after surgery was 0.0% and 63.6% for Type1 and Type 2 groups, respectively. Both Cobb angle of main curve and regional kyphosis were significantly corrected and well-maintained during follow-up (Table 2). The post-op CBD in Type 2 group didn't improve significantly (39.6±12.5mm vs. 33.6±18.7mm, p=0.380). However, this post-op CBD got compensated spontaneously during follow-up (33.6±18.7mm vs. 8.3±11.3mm, p=0.002).

Comparison between the balanced and imbalanced groups

The imbalanced group was assigned with 7 patients in total (46.7%), involving 0 patient from type 1 group, 2 patients from type 2A subgroup and 5 patients from type 2B subgroup. The total number of vertebrae distal to apex was larger in the balanced group (5.6±1.9 vs. 3.3±0.5, p=0.010). The pre and immediate post-op changes of the deformity parameters for both the upper and lower hemi-curves were shown in Table 3. The correction rate of CBD was significantly larger in the balanced group (78.4±25.1% vs. -22.9±29.7%, p<0.001), which was mirrored by better correction of UIV translation (71.6±35.5% vs. -5.8±32.1%, p<0.001). In the separate analysis for upper and lower hemi-curves, we found that the correction rate of the lower arc translation was significantly larger in the balanced group (59.1±12.9% vs. 44.9±7.9%, p<0.05). The correction of lower arc inclination was also larger in the balanced group but the difference didn't reach statistical significance (63.8±17.5% vs. 50.0±16.6%, p>0.05). As to the upper hemi-curve, over correction of the compensatory translation and inclination was more obvious with no statistical difference in the imbalanced group (70.9±248.6% vs. 29.7±33.7% and 225.9±292.8 vs. 23.3±47.0, p>0.05). Further comparative analysis revealed that both △UAT/△LAT and △UAI/△LAI were significant larger in the imbalanced group (△UAT/△LAT: 109.6±60.0% vs. 31.8±34.4%, p=0.008; △UAI/△LAI: 89.8±36.6% vs. 33.5±37.3%, p=0.012). These results were in line with the findings that the sum of

post-op UIV tilt + LIV tilt was significantly smaller in the balanced group (1.3±9.6° vs. 16.3±7.5°, p=0.005), neutralizing the coronal imbalance. It was also confirmed that both the UIV and the instrumentation mass tilted significantly to the convex side postoperatively in the imbalanced group (8.0±2.3° vs. -3.4±5.9°, p<0.001; 10.3±3.6° vs. 3.2±3.1°, p<0.001). Multiple linear regression analysis revealed that △UAT/△LAT (β=-21.567; p=0.018), but not △UAI/△LAI (β=-21.914; p=0.066), was significantly correlated with the correction of CBD.

Follow-up of the imbalanced group

Data of follow-up of the imbalanced group revealed spontaneous compensation of CCI (44.6±12.9mm vs. 12.6±9.6mm, p=0.002) (Ratio of CBD < 3 cm: 100%) (Table 4). Decreased tilting of the instrumentation mass and LIV to the convex side (distal compensation) (p<0.05) and increased UIV disc angle (proximal compensation) (p=0.095) accounted for such coronal rebalance. △UIV translation / △CBD (%) during follow-up averaged 63.3±36.2%, which revealed that distal compensation was the mainstay compensative mechanism.

Discussion

CCI associated with DS-NF1 is a unique subtype, and should be distinguished because of the prevailing dystrophic bone phenotype[16, 19, 20]. Strong distal screw purchases are the premise of coronal rebalance yet may not be obtainable for such patients. In this scenario, the management of CCI in DS-NF1 is challenging, especially for those with lower lumbar curve apex. Pelvic fixation can reliably improve the distal screw power, which was a key requirement for several innovative coronal realignment techniques[9, 11, 21, 22]. However, pelvic fixation is not popular for this young patient population. In order to resolve this dilemma, a relatively clear guideline is warranted.

The present study represented a homogeneous case series of dystrophic NF1 patients with convex trunk shift, and the incidence reached 8.4%. The newly developed classification showed the importance of distinguishing thoracic from thoracolumbar/lumbar CCI, as the incidence of immediate post-op CCI (≥3cm) was 0.0% and 63.6% for thoracic (Type1) and thoracolumbar/lumbar (Type 2) groups, respectively. This separation was essential because of its quite different prognosis. The likely mechanism was that the thoracic (Type1) CCI was usually associated with sufficient distal non-dystrophic pedicles and reliable distal screw purchases to achieve sufficient correction of distal fractional curve and subsequently a horizontal takeoff. For thoracolumbar/lumbar (Type 2) convex CI, limited and unreliable distal screw purchases were inclined to leave residual takeoff angle, increasing the risk of failure of coronal rebalance (Fig 5).

Further categorization according to the morphology of the upper hemi-curve was indicative of the compensational status and was instructional for correction maneuvers during surgery. The role of the lower hemi-curve was constant, being the coronal imbalance driver, while the role of the upper hemi-curve was switchable, from being straight & vertical to being curved & inclined, showing varied degrees of compensation. The quantitative comparative analysis revealed that mismatch between the upper and

lower hemi-curves in terms of correction of the arc translation and inclination existed and was prevailing in the imbalanced group. In other words, correction maneuvers in the upper hemi-curve region should be performed with caution to avoid over correction, Type 2 in particular.

The current classification was also treatment-oriented. A surgical rebalancing algorithm was proposed to treat each subtype (Table 5). For Type 1A patient, aggressive correction and verticality of the lower hemi-curve was essential, while concave distraction/convex compression maneuvers in upper hemi-curve region was optional, serving the role of fine-tuning for coronal realignment (Fig 6). For Type 1B patient, cooperative correction and verticality of the upper and lower hemi-curves should be performed, indicating concave distraction/convex compression for both ends (Fig 3). For Type 2A patient, an antagonistic rebalancing strategy was proposed: despite utmost correction of the lower hemi-curve being required, the verticality of the lower hemi-curve was usually suboptimal with poor distal screw strength, leaving residual takeoff angle. Fine-tuning using concave compression/convex distraction and coronal rod bending in upper hemi-curve region was beneficial to increase the coronal compensation (Fig 7). Opposite tilt of UIV and LIV with similar magnitude was required and should be visualized during surgery as a mark of relatively satisfying coronal rebalance. Clinicians should expect patient's self-rebalance over time if residual convex CI existed. For Type 2B patient, over correction of main curve was easy to occur, and thus cooperative correction was required. The degree of correction of the upper hemi-curve was determined and adjusted according to the correctability of the lower hemi-curve. Limited concave distraction/convex compression in upper hemi-curve was required to avoid over correction (Fig 4).

The follow-up data revealed that patients in the imbalanced group experienced spontaneous improvement of CCI over time (Ratio of CBD < 3 cm: 100%). This usually resulted in an acceptable but not satisfying coronal alignment because residual tilting of the instrumentation mass and/or junctional angulation centering around LIV existed (Fig 8), and might result in implant failure (Fig 5). Both distal compensation (decreased tilting of the instrumentation mass and LIV to the convex side) and proximal compensation (increased UIV disc angle) accounted for such coronal rebalance, and our data was suggestive that the distal compensation was the mainstay compensative mechanism. This was in line with Bao's previous finding that LIV at L4 or higher was correlated to a higher chance of spontaneous coronal rebalance[7].

The limitation for this study lied in that the sagittal alignment was not considered in the classification, which might also influence the design of surgical strategy.

Conclusion

The choice of coronal rebalance should be directed by the individual situation. This study presented a thought-provoking case series that illustrated the substantial utility of CCI classification, thereby, underlining its importance in designing personalized surgical tactic for patients with CCI in DS-NF1. This new classification should improve the recognition of the antagonistic roles of the upper and lower hemi-curves in the formation and correction of coronal imbalance. There also existed increasing difficulty of

correction of lower hemi-curve and increasing need for retaining upper hemi-curve compensation with descending apex location. In the event of CCI co-existing with poor limited distal screw purchases and utmost avoidance of pelvic fixation, cooperative correction between the upper and lower hemi-curve was essentially important. The lower hemi-curve should be corrected maximally while the upper hemi-curve played the role of fine-tuning for coronal realignment rather than radical Cobb correction, straight morphology in particular. It was impressive that the CCI had some relief during follow-up, beneficiating from both proximal and distal compensation. Sacrum or pelvic fixation should be taken as a salvage technique for potential instrumentation failure during follow-up.

Abbreviations

CCI: Convex coronal imbalance

DS-NF1: Dystrophic scoliosis secondary to Type I neurofibromatosis

UAT: Upper Arc Translation

LAT: Lower Arc Translation

TS: Trunk shift

CI: Coronal imbalance

DLS: degenerative lumbar scoliosis

CBD: Coronal balance distance

SVA: Sagittal vertical axis

CSVL: Center sacral vertical line

LAI: Lower arc inclination

UAI: Upper arc inclination

Declarations

Acknowledgments

Not applicable.

Authors' contributions

S.H.M, Z.Z.Z and Y.Q contributed to the design, conception, and revision of the article. S.L, Y.Y.M, B.L.S, and J.Q examined the patients and evaluated them clinically during follow-up. S.L and Z.L involved in

study design and data interpretation. All authors have read and approved the final manuscript.

Funding

This work has been founded by the Jiangsu Provincial Key Medical Center (YXZXA2016009)

Availability of data and materials

The datasets generated and/or analyzed during the current study are not publicly available but are available from the corresponding author on reasonable request.

Ethics approval and consent to participate

This study protocol was approved by the institutional review board of The Affiliated Hospital of Nanjing University Medical School (IRB No. 2017–112-08). Informed consent was obtained from the patients in this study. All methods were performed in accordance with the relevant guidelines and regulations.

Consent for publication

Not applicable.

Competing interests

The authors declare that they have no competing interests.

Author details

Division of Spine Surgery, Department of Orthopedic Surgery, Nanjing Drum Tower Hospital, The Affiliated Hospital of Nanjing University Medical School, Jiangsu, China

References

1. Crawford AH, Schorry EK (1999) Neurofibromatosis in children: the role of the orthopaedist. J Am Acad Orthop Surg 7:217-230. doi: 10.5435/00124635-199907000-00002
2. Vitale MG, Guha A, Skaggs DL (2002) Orthopaedic manifestations of neurofibromatosis in children: an update. Clin Orthop Relat Res:107-118. doi: 10.1097/00003086-200208000-00013
3. Durrani AA, Crawford AH, Chouhdry SN, Saifuddin A, Morley TR (2000) Modulation of spinal deformities in patients with neurofibromatosis type 1. Spine (Phila Pa 1976) 25:69-75. doi: 10.1097/00007632-200001010-00013
4. Maier SP, Smith JS, Schwab FJ, Obeid I, Mundis GM, Klineberg E, Hostin R, Hart RA, Burton D, Boachie-Adjei O, Gupta M, Ames C, Protopsaltis TS, Lafage V, International Spine Study G (2014) Revision Surgery After 3-Column Osteotomy in 335 Patients With Adult Spinal Deformity: Intercenter Variability and Risk Factors. Spine (Phila Pa 1976) 39:881-885. doi: 10.1097/BRS.0000000000000304

5. Glassman SD, Berven S, Bridwell K, Horton W, Dimar JR (2005) Correlation of radiographic parameters and clinical symptoms in adult scoliosis. Spine (Phila Pa 1976) 30:682-688. doi: 10.1097/01.brs.0000155425.04536.f7
6. Cho W, Mason JR, Smith JS, Shimer AL, Wilson AS, Shaffrey CI, Shen FH, Novicoff WM, Fu KM, Heller JE, Arlet V (2013) Failure of lumbopelvic fixation after long construct fusions in patients with adult spinal deformity: clinical and radiographic risk factors: clinical article. J Neurosurg Spine 19:445-453. doi: 10.3171/2013.6.SPINE121129
7. Bao H, Yan P, Qiu Y, Liu Z, Zhu F (2016) Coronal imbalance in degenerative lumbar scoliosis: Prevalence and influence on surgical decision-making for spinal osteotomy. Bone Joint J 98-B:1227-1233. doi: 10.1302/0301-620X.98B9.37273
8. Obeid I, Berjano P, Lamartina C, Chopin D, Boissiere L, Bourghli A (2019) Classification of coronal imbalance in adult scoliosis and spine deformity: a treatment-oriented guideline. Eur Spine J 28:94-113. doi: 10.1007/s00586-018-5826-3
9. Bao H, Liu Z, Zhang Y, Sun X, Jiang J, Qian B, Mao S, Qiu Y, Zhu Z (2019) Sequential correction technique to avoid postoperative global coronal decompensation in rigid adult spinal deformity: a technical note and preliminary results. Eur Spine J 28:2179-2186. doi: 10.1007/s00586-019-06043-9
10. Makhni MC, Zhang Y, Park PJ, Cerpa M, Yang M, Pham MH, Sielatycki JA, Beauchamp EC, Lenke LG (2019) The "kickstand rod" technique for correction of coronal imbalance in patients with adult spinal deformity: initial case series. J Neurosurg Spine:1-8. doi: 10.3171/2019.9.SPINE19389
11. Redaelli A, Langella F, Dziubak M, Cecchinato R, Damilano M, Peretti G, Berjano P, Lamartina C (2020) Useful and innovative methods for the treatment of postoperative coronal malalignment in adult scoliosis: the "kickstand rod" and "tie rod" procedures. Eur Spine J. doi: 10.1007/s00586-019-06285-7
12. Jain A, Hassanzadeh H, Strike SA, Menga EN, Sponseller PD, Kebaish KM (2015) Pelvic Fixation in Adult and Pediatric Spine Surgery: Historical Perspective, Indications, and Techniques: AAOS Exhibit Selection. The Journal of bone and joint surgery American volume 97:1521-1528. doi: 10.2106/JBJS.O.00576
13. Dayer R, Ouellet JA, Saran N (2012) Pelvic fixation for neuromuscular scoliosis deformity correction. Curr Rev Musculoskelet Med 5:91-101. doi: 10.1007/s12178-012-9122-2
14. Kurucan E, Bernstein DN, Thirukumaran C, Jain A, Menga EN, Rubery PT, Mesfin A (2018) National Trends in Spinal Fusion Surgery for Neurofibromatosis. Spine Deform 6:712-718. doi: 10.1016/j.jspd.2018.03.012
15. Akbarnia BA, Gabriel KR, Beckman E, Chalk D (1992) Prevalence of scoliosis in neurofibromatosis. Spine (Phila Pa 1976) 17:S244-248. doi: 10.1097/00007632-199208001-00005
16. Kim HW, Weinstein SL (1997) Spine update. The management of scoliosis in neurofibromatosis. Spine (Phila Pa 1976) 22:2770-2776. doi: 10.1097/00007632-199712010-00014
17. Jia F, Cui X, Wang G, Liu X, Sun J (2019) Spontaneous rotational dislocation of the lumbar spine in type 1 neurofibromatosis: A case report and literature review. Medicine (Baltimore) 98:e15258. doi: 10.1097/MD.0000000000015258

18. Tsirikos AI, Dhokia R, Wordie S (2018) Rotatory Dislocation of the Spine in Dystrophic Kyphoscoliosis Secondary to Neurofibromatosis Type 1. J Cent Nerv Syst Dis 10:1179573518819484. doi: 10.1177/1179573518819484
19. Prudhomme L, Delleci C, Trimouille A, Chateil JF, Prodhomme O, Goizet C, Van Gils J (2020) Severe Thoracic and Spinal Bone Abnormalities in neurofibromatosis type 1. Eur J Med Genet 63:103815. doi: 10.1016/j.ejmg.2019.103815
20. Wang Z, Liu Y (2010) Research update and recent developments in the management of scoliosis in neurofibromatosis type 1. Orthopedics 33:335-341. doi: 10.3928/01477447-20100329-20
21. Buell TJ, Buchholz AL, Mazur MD, Mullin JP, Chen CJ, Sokolowski JD, Yen CP, Shaffrey ME, Shaffrey CI, Smith JS (2019) Kickstand Rod Technique for Correcting Coronal Imbalance in Adult Scoliosis: 2-Dimensional Operative Video. Oper Neurosurg (Hagerstown). doi: 10.1093/ons/opz306
22. Makhni MC, Cerpa M, Lin JD, Park PJ, Lenke LG (2018) The "Kickstand Rod" technique for correction of coronal imbalance in patients with adult spinal deformity: theory and technical considerations. J Spine Surg 4:798-802. doi: 10.21037/jss.2018.11.04

Tables

Table 1 Summary of surgical strategies

Surgical strategies	Type 1 (4)	Type 2 (11)
PSF	1	8
Skull-Femoral Traction + PSF	1	0
Halo Gravity Traction + PSF	1	0
PSF+ASF	0	2
Halo Gravity Traction + PSF + ASF	1	0
Anterior release + Skull-Femoral Traction + PSF	0	1
Ratio of traction (%)	75%	9.1%
Ratio of combined approach (%)	25%	27.3%

PSF: posterior spinal fusion, ASF: anterior supplemental fusion

Table 2 Data of deformity correction, dystrophic characteristics and instrumentation constructs for the Type 1 and Type 2 groups

Parameters	Type 1	Type 2
Main curve (°)		
Pre	86.2±23.9	60.6±20.4
Post	44.9±13.9	23.7±14.0
Latest FU	42.9±9.7	24.0±14.3
Kyphosis (°)		
Pre	77.5±15.5	37.6±13.2
Post	31.1±4.1	-0.7±16.8
Latest FU	29.4±5.0	-0.5±17.5
CBD (mm)		
Pre	54.4±12.8	39.6±12.5
Post	5.4±11.6	33.6±18.7
Latest FU	1.3±5.8	8.3±11.3
SVA (mm)		
Pre	-20.1±43.8	-35.6±25.2
Post	22.1±26.3	-18.0±29.9
Latest FU	3.5±26.8	-17.9±33.3
Postoperative CI	0%	63.6%
Number of dystrophic segments	5.3±1.0	4.6±1.0
VRS	3 (75%)	9 (81.8%)
Fusion segments	11.8±1.0	8.5±1.5
Implant density (%)	67.7±3.1	78.0±13.2
Laminar hook ratio (%)	11.2±11.5	9.7±16.4

CBD: coronal balance distance, SVA: sagittal vertical axis, CI: coronal imbalance, VRS: vertebral rotatory subluxation

Table 3 Comparative analysis between the balanced and imbalanced groups

	Balanced group (n=8)	Imbalanced group (n=7)	p
CBD (mm)			
Preoperative	49.0±13.0	37.3±12.9	0.105
Postoperative	9.9±10.5	44.6±12.9	<0.001
Correction rate (%)	78.4±25.1	-22.9±29.7	<0.001
UAI (°)			
Preoperative	-22.7±11.9	-10.3±5.5	0.026
Postoperative	-13.3±5.3	3.2±5.1	<0.001
Correction rate (%)	23.3±47.0	225.9±292.8	0.075
△UAI	9.1±9.1	13.5±6.4	0.330
LAI (°)			
Preoperative	49.6±8.7	31.2±6.9	0.001
Postoperative	18.3±9.4	14.8±2.3	0.348
Correction rate (%)	63.8±17.5	50.0±16.6	0.141
△LAI	-31.2±8.8	-16.4±7.8	0.005
△UAI/△LAI (%)	33.5±37.3	89.8±36.6	0.012
UAT (mm)			
Preoperative	-38.5±18.9	-15.8±13.4	0.021
Postoperative	-22.9±11.5	7.8±8.3	<0.001
Correction rate (%)	29.7±33.7	70.9±248.6	0.649
△UAT	15.6±13.1	23.7±10.2	0.211
LAT (mm)			
Preoperative	86.5±20.1	50.6±9.9	0.001
Postoperative	35.2±12.8	27.6±3.9	0.157
Correction rate (%)	59.1±12.9	44.9±7.9	0.024
△LAT	-51.3±17.0	-23.0±7.6	0.001
△UAT/△LAT(%)	31.8±34.4	109.6±60.0	0.008
Instrumentation mass inclination (°)			
Preoperative	14.7±4.7	8.5±3.4	0.013

Postoperative	3.2±3.1	10.3±3.6	0.001
Correction rate (%)	74.3±33.5	-30.0±33.5	<0.001
LIV tilt (°)			
Preoperative	21.0±13.0	19.2±7.6	0.754
Postoperative	4.6±6.6	8.3±7.0	0.316
Correction rate (%)	73.2±38.9	72.2±64.7	0.971
UIV tilt (°)			
Preoperative	-9.5±7.7	-0.7±8.1	0.049
Postoperative	-3.4±5.9	8.0±2.3	<0.001
Correction rate (%)	153.3±285.0	-109.4±652.8	0.320
UIV translation (mm)			
Preoperative	48.0±14.3	34.7±6.9	0.045
Postoperative	12.3±13.1	35.4±6.9	0.001
Correction rate (%)	71.6±35.5	-5.8±32.1	0.001
UIV tilt + LIV tilt (°)			
Preoperative	11.5±13.0	18.6±9.9	0.257
Postoperative	1.3±9.6	16.3±7.5	0.005

UAI: Upper arc inclination, LAI: Lower arc inclination, UAT: Upper arc translation, LAT: Lower arc translation, LIV: Lower instrumented vertebra, UIV: Upper instrumented vertebra

Table 4 Follow-up data of the imbalanced group

	Postoperative	Latest FU	*p
Main curve (°)	17.0±7.2	16.9±8.3	0.894
Kyphosis (°)	0.0±10.7	0.3±12.6	0.975
Coronal balance (mm)	44.6±12.9	12.6±9.6	0.002
Instrumentation mass inclination (°)	10.3±3.6	4.7±3.4	<0.001
UIV translation	35.4±6.9	16.3±8.5	0.002
UIV disc angle	1.6±1.5	5.1±5.1	0.095
LIV tilt	8.3±7.0	1.0±7.6	0.008
Ratio of CBD < 3 cm	-----	100%	----
△UIV translation / △CBD (%)	-----	63.3±36.2	----

LIV: Lower instrumented vertebra, UIV: Upper instrumented vertebra, CBD: coronal balance distance

Table 5 The surgical rebalancing algorithm for each subtype

Main types	Subtypes	Main features	Corrective maneuvers for coronal rebalance
Type 1 Thoracic (Apex of main curve above T12)	Type 1A No compensation of the upper hemi-curve	Morphology of the upper hemi-curve being straight & vertical; Sufficient non-dystrophic distal pedicles (≥3)	Aggressive correction and verticality of the lower hemi-curve; No significant concave distraction/convex compression in upper hemi-curve; Fine-tuning of upper hemi-curve for coronal realignment
	Type 1B Obvious coronal compensation of the upper hemi-curve	Morphology of the upper hemi-curve being obviously curved & inclined; Sufficient non-dystrophic distal pedicles (≥3)	Cooperative correction and verticality of the upper and lower hemi-curves (concave distraction/convex compression for both ends)
Type 2 Thoracolumbar/Lumbar (Apex of main curve between T12 and L4)	Type 2A No compensation of the upper hemi-curve	Morphology of the upper hemi-curve being straight & vertical; Limited (Thoracolumbar) or insufficient (Lumbar) non-dystrophic distal pedicles (≤3)	Antagonistic strategy: utmost correction of the lower hemi-curve; Verticality of the lower hemi-curve usually being suboptimal with poor distal screw strength; Fine-tuning using concave compression/convex distraction and coronal rod bending in upper hemi-curve to increase the coronal compensation; Opposite tilt of UIV and LIV with similar magnitude; Expect patient's self-rebalance over time if residual CCI exists.
	Type 2B Obvious coronal compensation of the upper hemi-curve	Morphology of the upper hemi-curve being obviously curved & inclined; Limited (Thoracolumbar) or insufficient (Lumbar) non-dystrophic distal pedicles (≤3)	Cooperative correction of the upper and lower hemi-curves (restrict the correction of upper hemi-curve, limited concave distraction/convex compression in upper hemi-curve); Utmost correction of the lower hemi-curve; Opposite tilt of UIV and LIV with similar magnitude; Expect patient's self-rebalance over time if residual CCI exists.

Figures

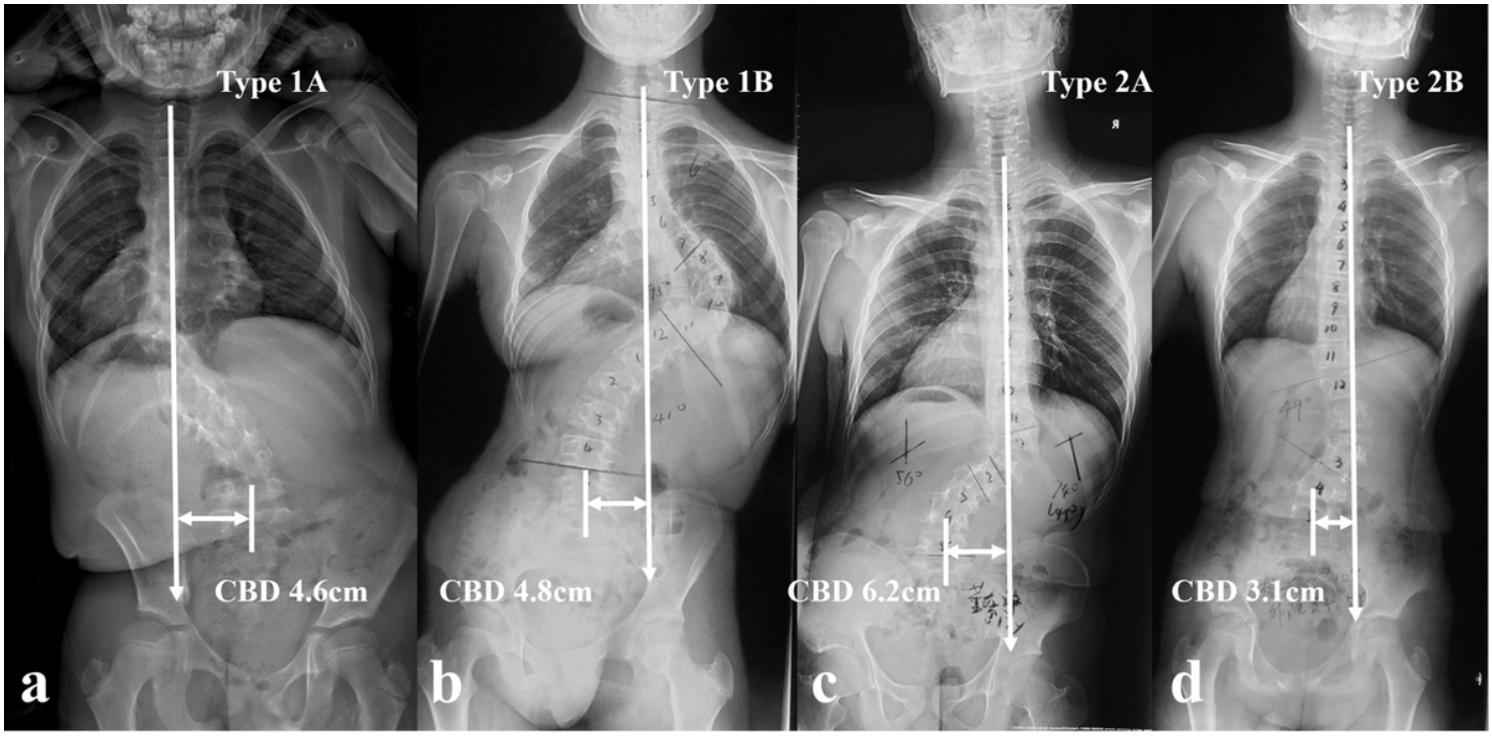

Figure 1

Illustration of the classification of CCI in DS-NF1: a, Type 1A; b, Type 1B; c, Type 2A; d, Type 2B.

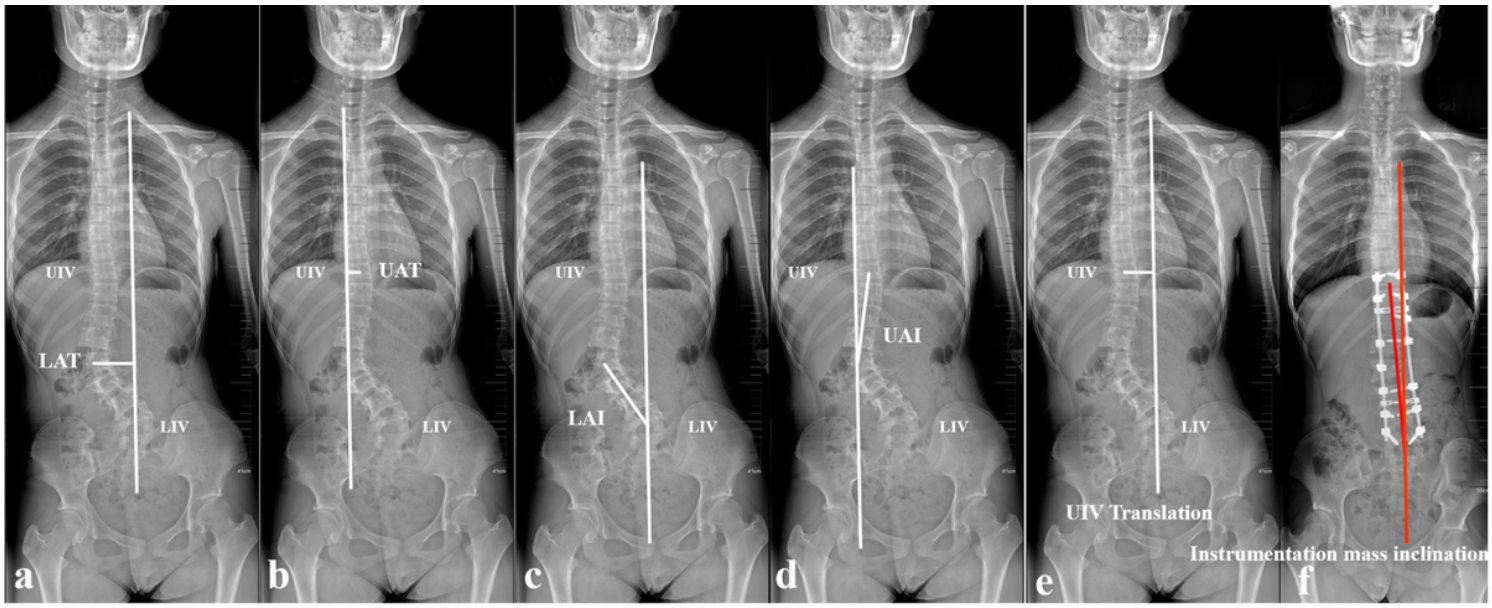

Figure 2

Illustration of the measurements of the lower arc translation (LAT, a), upper arc translation (UAT, b), lower arc inclination (LAI, c), upper arc inclination (UAI, d), UIV translation (e), instrumentation mass inclination (f).

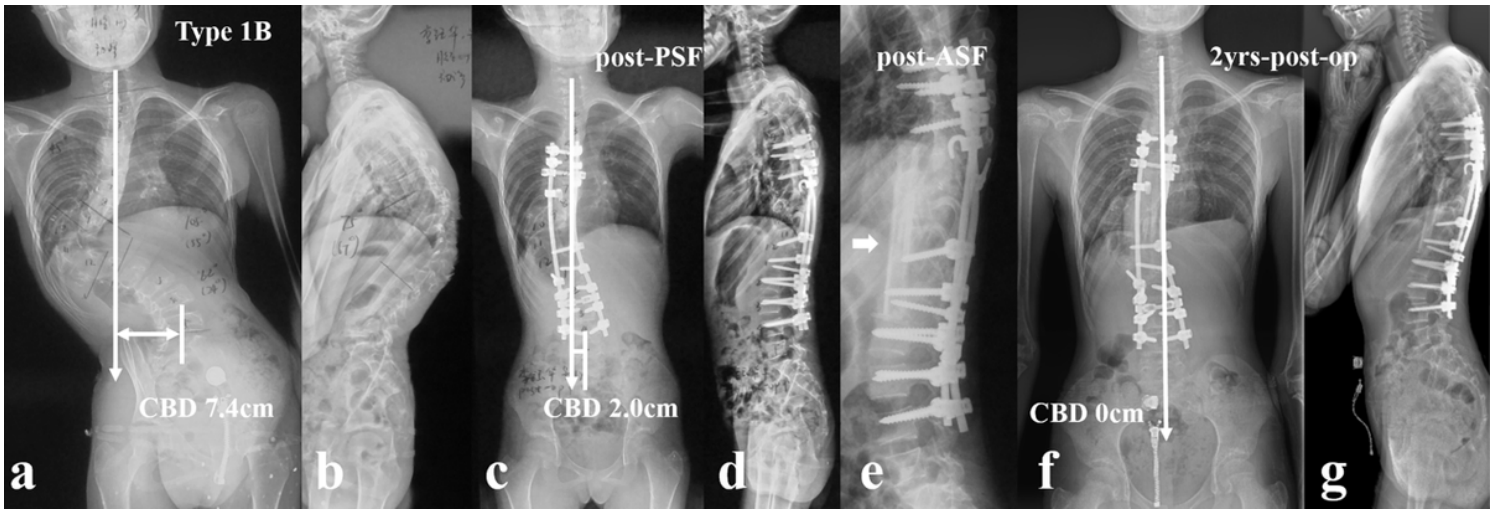

Figure 3

Type 1B an 11-year-old girl with NF1, suffering from kyphoscoliosis associated with convex trunk shift and dystrophic vertebral rotatory subluxation at T9/10 level (a, b); Halo Gravity Traction on wheelchair was prescribed for one month. Afterwards, stage 1 posterior spinal correction and fusion surgery was performed (c, d), followed by stage 2 supplementary anterior fusion utilizing structural fibular allograft (e, arrow). 2-year-follow up revealed spontaneous improvement of coronal balance with solid fusion (f, g).

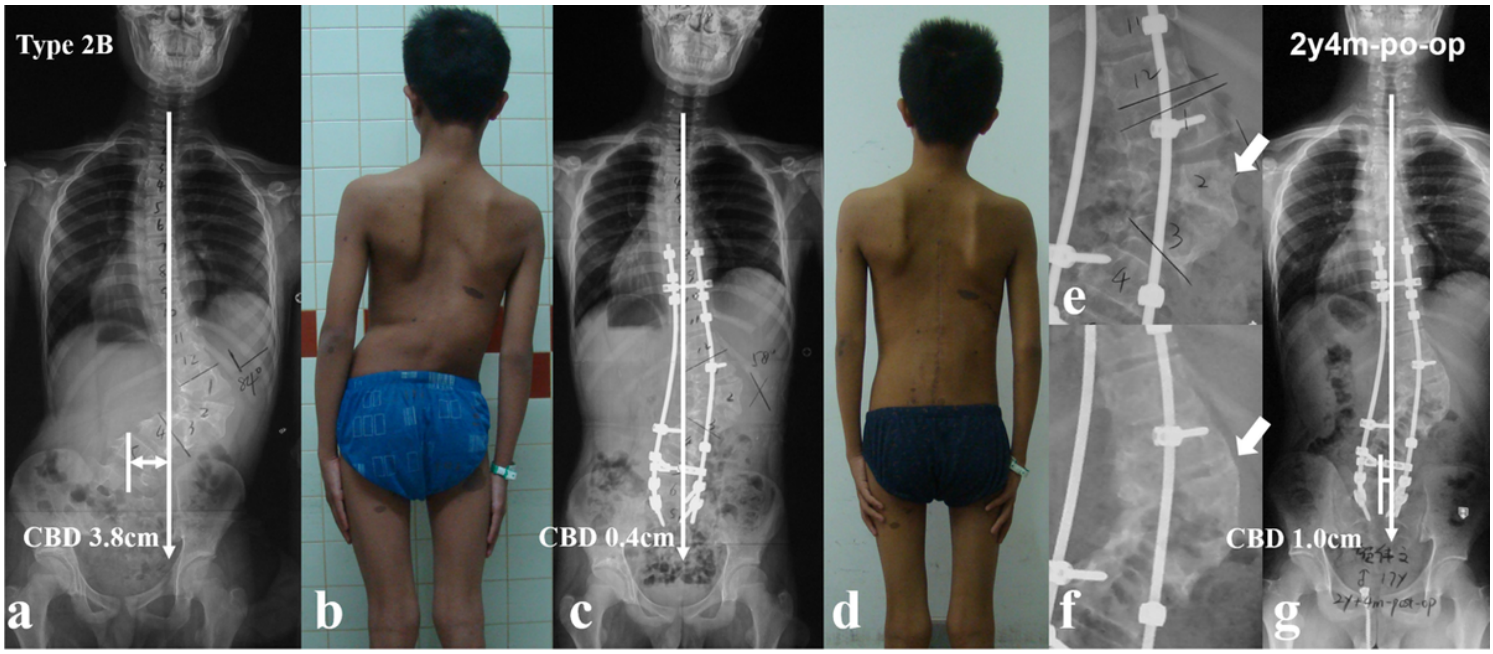

Figure 4

Type 2B a 17-year-old boy with NF1 related lumbar kyphoscoliosis associated with CCI and dystrophic vertebral rotatory subluxation at L2/3 & L3/4 levels (a, b). Stage 1 posterior spinal correction and fusion surgery was performed with low screw density yet with generous posterior fusion, followed by stage 2 supplementary anterior intervertebral fusion utilizing autogenous rib grafts (c, e). The coronal balance was well reconstructed despite low correction rate of main curve (d). 2.25-year-follow up revealed

satisfying intervertebral fusion (f) and well maintenance of coronal balance with no instrumentation failure (g).

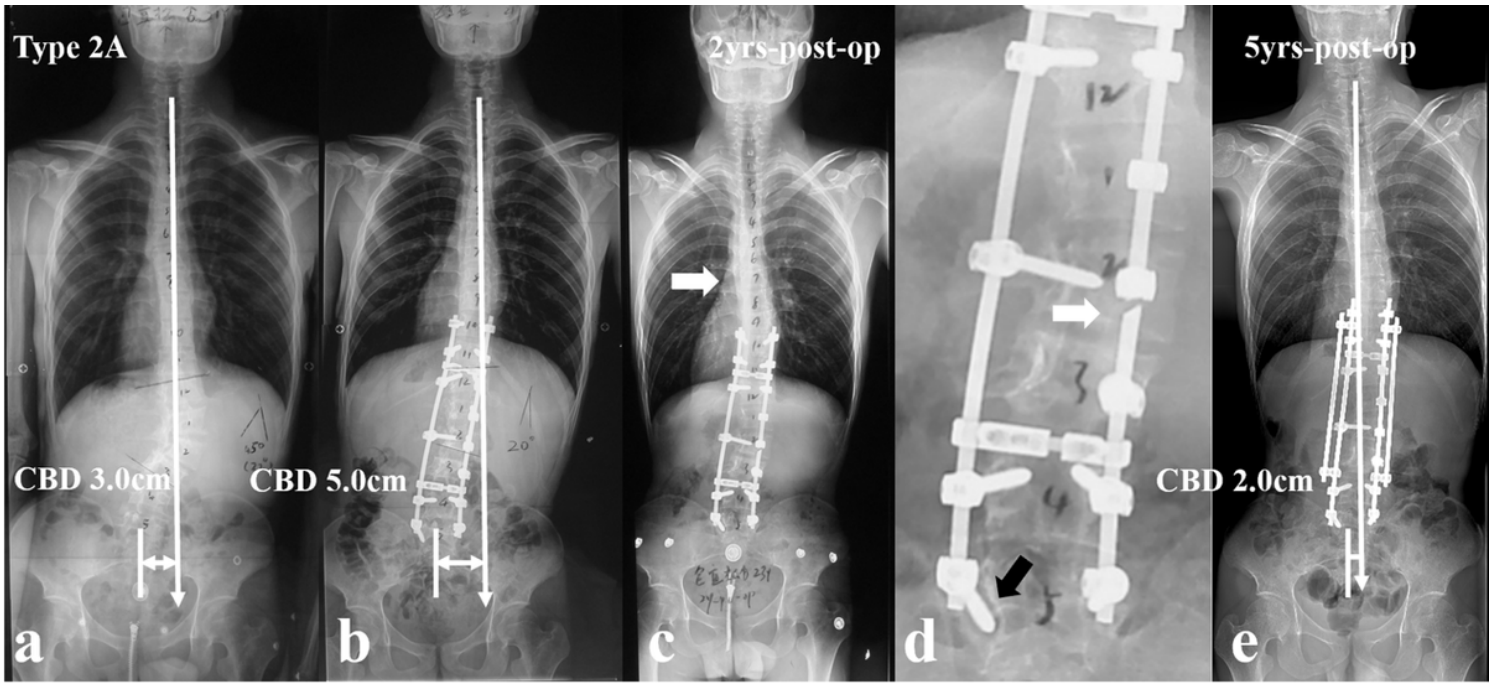

Figure 5

Type 2A a 26-year-old male patient with NF1 related lumbar kyphoscoliosis associated with CCI (a). Posterior spinal correction and fusion surgery was performed with suboptimal correction of lower hemi-curve and over correction of upper hemi-curve, resulting in iatrogenic aggravation of CCI (b). Despite spontaneous improvement of CCI during follow-up (c), rod fracture occurred at 2-year-follow up (d, arrow). Revision surgery was performed with satellite rods (four rod constructs) and generous posterior fusion, and no additional rod fracture occurred by 5-year-follow up.

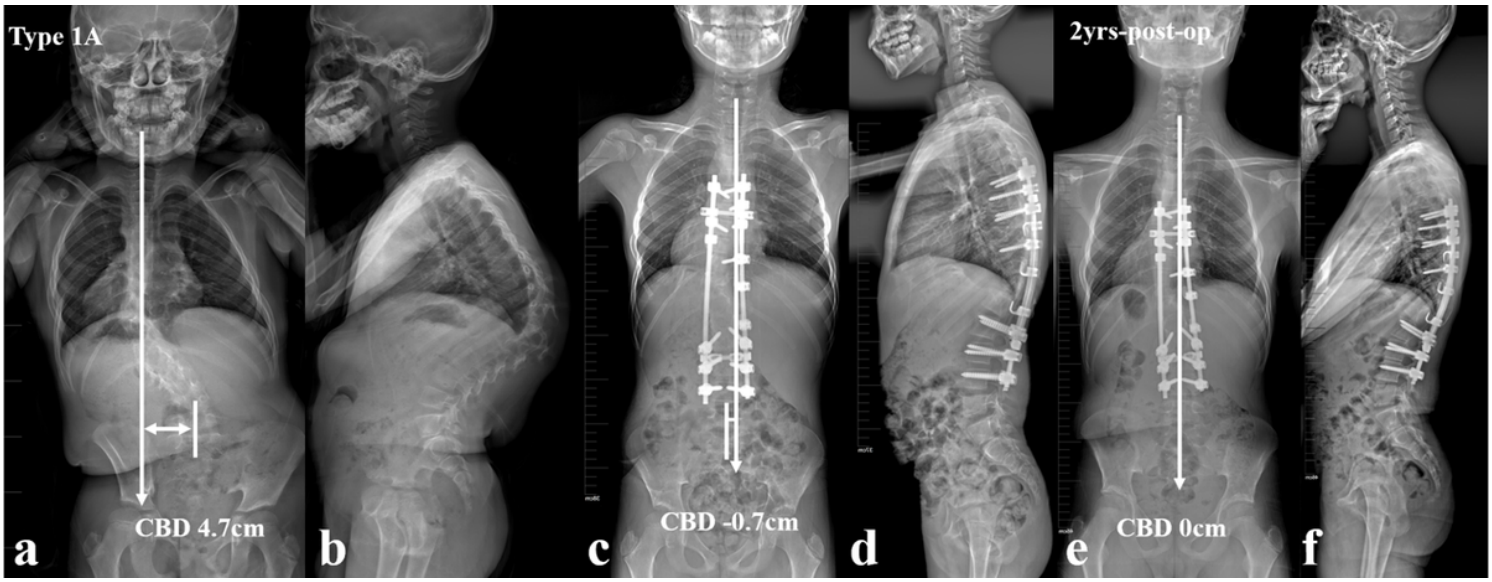

Figure 6

Type 1A a 12-year-old boy with NF1 related thoracic kyphoscoliosis associated with CCI (a, b). Halo gravity traction on wheelchair was prescribed for one month. Afterwards, posterior spinal correction and fusion surgery was performed (c, d), and the CCI improved from 4.7cm to -0.7cm postoperatively (c, d). At 2-year-follow up, the CBD got further improvement to 0 cm (e, f).

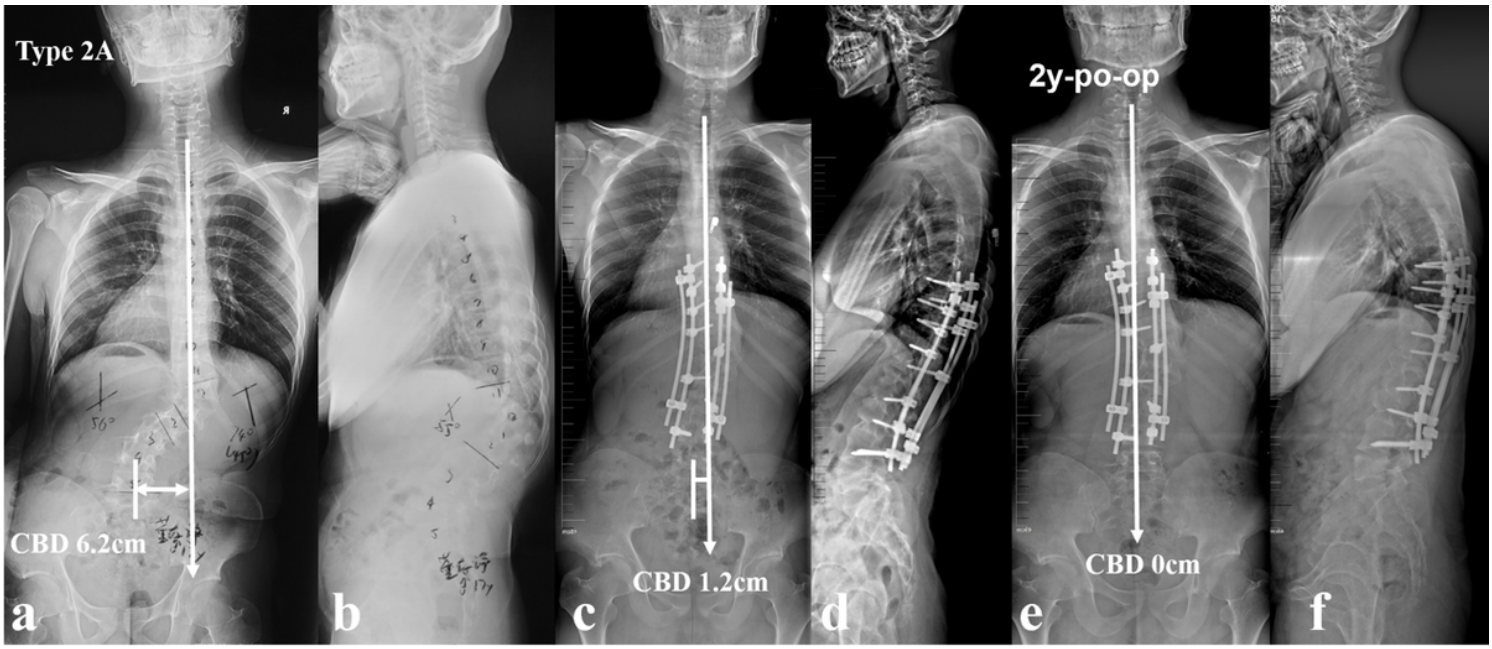

Figure 7

Type 2A a 17-year-old boy with NF1 related thoracolumbar kyphoscoliosis associated with CCI and vertical straight morphology of upper hemi curve (a, b). Antagonistic strategy was applied with utmost correction of the lower hemi-curve. Verticality of the lower hemi-curve was suboptimal. Fine-tuning using concave compression/convex distraction and coronal rod bending in upper hemi-curve was performed to increase the coronal compensation, resulting in opposite tilt of UIV and LIV with similar magnitude (c, d). At 2-year-follow up, the CBD got further improvement to 0 cm (e, f).

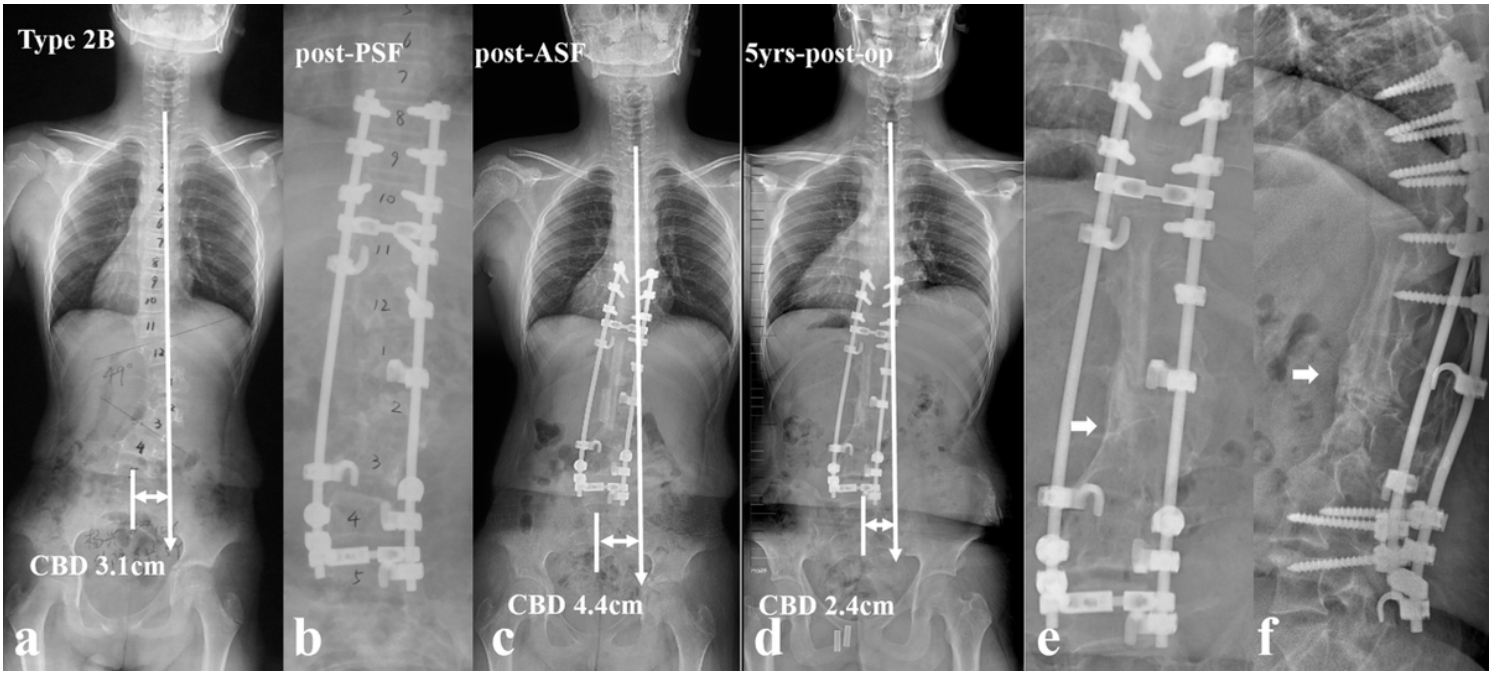

Figure 8

Type 2B an 11-year-old boy with NF1 related lumbar kyphoscoliosis associated with CCI (a); Stage 1 posterior spinal correction and fusion surgery using hybrid implants (screws and hooks) was performed with low screw density at apical region (b), followed by stage 2 supplementary anterior intervertebral fusion utilizing structural fibular allograft (c). Over correction of upper hemi curve resulted in aggravation of CCI. The patient experienced spontaneous improvement of CBD at 5 years follow-up (d). Despite low implant density, no implant failure occurred because the fusion of the anterior column was good (e, f).